Multicoated gratings: a differential formalism applicable in the entire optical region

J. Chandezon, M. T. Dupuis, and G. Cornet

Laboratoire de Radioélectricité, Greco Centre National de la Recherche Scientifique No. 11, Université de Clermont-Ferrand II, B.P. 45, 63170 Aubiere, France

D. Maystre

Laboratoire d'Optique Electromagnétique, Equipe de Recherche Associée au Centre National de la Recherche Scientifique No. 597, Faculté des Sciences et Techniques, Centre de St-Jérôme, 13397 Marseille Cedex 13, France

Received November 5, 1981

We present a new formalism for the diffraction of an electromagnetic plane wave by a multicoated grating. Its basic feature lies in the use of a coordinate system that maps all the interfaces onto parallel planes. Using Maxwell's equations in this new system leads to a linear system of differential equations with constant coefficients whose solution is obtained through the calculation of the eigenvalues and eigenvectors of a matrix in each medium. Through classical criteria, our numerical results have been found generally to be accurate to within 1%. The serious numerical difficulties encountered by the previous differential formalism for highly conducting metallic gratings completely disappear, whatever the optical region. Furthermore, our computer code provides accurate results for metallic gratings covered by many modulated dielectric coatings or for highly modulated gratings. We give two kinds of applications. The first concerns the use of dielectric coatings on a modulated metallic substrate to minimize the absorption of energy. Conversely, the second describes the use of highly modulated metallic gratings to increase this absorption.

1. INTRODUCTION

Nowadays, rigorous solutions of the grating diffraction problem are well known. Schematically, they can be classified in two types according to their use of integral or differential methods.[1] This classification is still valid for multicoated gratings, i.e., gratings covered by a certain number of dielectric or metallic layers. However, numerical instabilities encountered so far in the differential methods are such that only the integral method is able to give correct results in the visible and infrared regions.

In this paper, we propose a differential formalism that works in the whole domain of optics. It consists of a generalization of the formalism already proposed for a perfectly conducting uncoated grating[2] to the multicoated grating. We use Maxwell's equations in covariant form[3] in a nonorthogonal system of coordinates fitted to the grating geometry. The originality of our differential formalism lies chiefly in the fact that the coefficients of the infinite system of coupled differential equations are constant. This fundamental feature enables us to reduce the numerical solution of the problem to finding the eigenvalues and eigenvectors of a matrix in every layer. Classical numerical tests show that the precision is of the order of 10^{-3}. We have been able to reproduce the previous results of Maystre *et al.*[4] for the improvement of the aluminum grating efficiency obtained by depositing adequate dielectric coatings on the metallic substrate. Precision problems in the evaluation of the eigenvalues and eigenvectors prevent us from achieving the computations when the total thickness of dielectric exceeds one wavelength, or when the number of layers exceeds eight, but these limitations could be modified by using more-sophisticated numerical techniques. This method enables one, for the first time to our knowledge, to study a grating covered by a great number of layers separated by modulated interfaces. This could be of great interest for use both in the visible (gratings used at the end of a laser cavity[4,5]) and in the infrared (sampling mirrors for high-power lasers[5]).

2. PRESENTATION OF THE PROBLEM AND NOTATION

The metallic or dielectric substrate, with complex index ν_0, is covered by Q dielectric or metallic layers with indices ν_j and thicknesses e_j (Fig. 1), the total thickness of the coating being $e = \sum_{j=1}^{Q} e_j$. The grating is illuminated in vacuum (medium $Q + 1$) by a homogeneous monochromatic plane wave with angle of incidence θ, with a wave vector $\mathbf{k}$ ($k = |\mathbf{k}| = 2\pi/\lambda$), situated in the $0xy$ plane, λ being the wavelength in vacuum.

The upper interface is given in the $0xyz$ axes by the equation $y = a(x)$, where $a(x)$ is periodic in x with period $d = 2\pi/K$. So the upper limit of the jth medium (of index ν_j) is given by $y = a(x) + u_j$, where $u_j = -\sum_{i=j+1}^{Q} e_j$, u_0 thus being equal to $-e$ and u_Q equal to 0.

We classically distinguish the two fundamental cases of polarization, called TE or TM according to whether the electric field or the magnetic field remains parallel to the $0z$ axis. To simplify the notation, we call F^i the complex amplitude of the incident field, equal to ${E_z}^i$ (TE case) or ${H_z}^i(\mu_0/\epsilon_0)^{1/2}$ (TM case), where ${E_z}^i$ and ${H_z}^i$ denote the complex amplitudes of the only component (parallel to $0z$) of the

0030-3941/82/070839-08$01.00

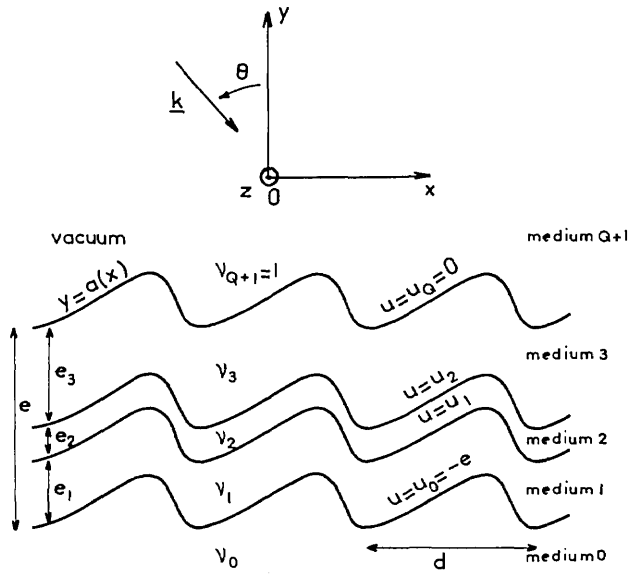

Fig. 1. Presentation of the problem and notation for a total number of layers $Q = 3$.

incident electric or magnetic field. We normalize this incident field by writing

$$F^i = \exp(ikx \sin\theta - iky \cos\theta), \tag{1}$$

where the time dependence $\exp(-i\omega t)$ is omitted. The problem, for the two cases of polarization, is to determine the total field F, equal to E_z (TE case) or $H_z(\mu_0/\epsilon_0)^{1/2}$ (TM case). We define the diffracted field F^d in vacuum by $F^d = F - F^i$.

From the fundamental laws of electromagnetism, it can be shown that this physical problem of diffraction leads to a boundary problem for the fields, which must satisfy[1]

(1) Maxwell's equations in each homogeneous medium;
(2) Boundary conditions on each interface;
(3) An outgoing wave condition (OWC) when $y \to \pm\infty$.

The third condition means that the diffracted field must propagate upward and remain finite when $y \to \infty$ and that the total field must propagate downward and remain finite when $y \to -\infty$.

From these conditions, it can be shown that, above the grooves, i.e., when $y > \max[a(x)]$, the diffracted field can be represented by a plane-wave expansion[1]:

$$F^d = \sum_n B_n \exp[i(\alpha_n x + \beta_n y)], \tag{2}$$

with

$$\alpha_n = k \sin\theta + nK, \tag{3}$$

where

$$\beta_n = (k^2 - \alpha_n{}^2)^{1/2} \quad \text{if} \quad n \in U,$$

$$\beta_n = i(\alpha_n{}^2 - k^2)^{1/2} \quad \text{if} \quad n \notin U,$$

U being the set of P integers such that $|\alpha_n| < k$, and Σ_n denoting a sum from $n = -\infty$ to $n = +\infty$.

It is worth noting that the right-hand side of Eq. (2) contains two parts that are different in nature from a physical point of view. The first part, which we call the asymptotic diffracted field F^{ad}, is equal to the sum of the finite number of terms corresponding to $n \in U$. The other part of the diffracted field, corresponding to $n \notin U$, defines the evanescent diffracted field F^{ed} that can be neglected when $y \to \infty$. So the asymptotic diffracted field F^{ad} is a sum of homogeneous plane waves whose directions of propagation can be derived from Eq. (3) by defining the diffraction angles $\theta_n = \arcsin(\alpha_n/k)$:

$$\sin\theta_n = \sin\theta + n\lambda/d.$$

We know that the plane-wave expansion described by Eq. (2) generally cannot describe the field inside the grooves. However, we will define the asymptotic diffracted field in vacuum as a plane-wave expansion, even inside the grooves. If $a(x) \leqslant y \leqslant \mathrm{Max}[a(x)]$,

$$F^{ad} = \sum_{n \in U} B_n \exp[i(\alpha_n x + \beta_n y)]; \tag{4}$$

so the relation in vacuum

$$F^d = F^{ad} + F^{ed} \tag{5}$$

becomes, for $a(x) \leqslant y \leqslant \mathrm{Max}[a(x)]$, a definition of F^{ed}, which, of course, cannot be represented, in general, by a plane-wave expansion. Equations (4) and (5), which are one of the novelties of our formalism and which, in the following, will be efficient from a numerical point of view, should not be confused with the inexact considerations of the Rayleigh expansion method,[1] which considers that the whole diffracted field can be described by a plane-wave expansion.

The fundamental question for the user is to know the efficiencies $\mathcal{E}_n$, defined for $n \in U$ as the energy diffracted in the nth order divided by the incident energy ratios. Bearing in mind that the incident wave has a unit amplitude, it can be shown[1] that

$$\mathcal{E}_n = B_n B_n{}^* \cos\theta_n/\cos\theta,$$

where the asterisk denotes the complex conjugate.

3. THEORETICAL STUDY

A. Translation Coordinate System

To be able to write in a simple manner the continuity conditions of the electromagnetic field on the interfaces, it is convenient to use those interfaces as coordinate surfaces. The fundamental feature of our method is to use the simplest of these coordinate systems, which we call the translation system, in which y is replaced by u, defined by

$$u = y - a(x),$$

the coordinates x and z being unchanged.[2,6]

B. Expressions of F^i and F^{ad} in the New Coordinate System

In the new system, the expression for the incident field becomes, for $u \geqslant 0$,

$$F^i = \exp(-iku \cos\theta)\exp[-ika(x)\cos\theta]\exp(ikx \sin\theta).$$

That is, developing in a Fourier series the second exponential of the right-hand member,

$$F^i = \sum_m L_m(\beta_0)\exp[i(\alpha_m x - \beta_0 u)], \tag{6}$$

with

$$L_m(t) = \frac{1}{d}\int_0^d \exp\{-i[a(x)t + mKx]\}dx. \quad (7)$$

In the same way, the asymptotic diffracted field can be written as

$$F^{ad} = \sum_{n\in U}\sum_m B_n L_{m-n}(-\beta_n)\exp[i(\alpha_m x + \beta_n u)]. \quad (8)$$

C. Stating Maxwell's Equations and the Boundary Condition

In addition to F, we define another covariant component G of the fields such that, in the jth medium,

$$F = E_z, \qquad G = kZ_0H_x \qquad \text{for TE polarization,}$$
$$F = Z_0H_z, \qquad G = -k\nu_j^2E_x \qquad \text{for TM polarization,}$$

with $Z_0 = (\mu_0/\epsilon_0)^{1/2}$.

Thanks to these notations, Maxwell's equations in covariant form[3,6] permit us to derive a system of partial differential equations of the first order in u, independently of the polarization:

$$\frac{\partial F}{\partial u} = \frac{a'}{1+a'^2}\frac{\partial F}{\partial x} + \frac{i}{1+a'^2}G, \quad (9)$$

$$\frac{\partial G}{\partial u} = \frac{\partial}{\partial x}\left(\frac{i}{1+a'^2}\frac{\partial F}{\partial x}\right) + i\nu_j^2k^2F + \frac{\partial}{\partial x}\left(\frac{a'}{1+a'^2}G\right), \quad (10)$$

where a' denotes the derivative of $a(x)$ with respect to x.

Now introduction of the vector ψ whose components are two functions,

$$\psi = \begin{pmatrix} F \\ G \end{pmatrix} = \begin{pmatrix} E_z \\ kZ_0H_x \end{pmatrix} \text{ for TE polarization,}$$
$$\psi = \begin{pmatrix} F \\ G/\nu_j^2 \end{pmatrix} = \begin{pmatrix} Z_0H_z \\ -kE_x \end{pmatrix} \text{ for TM polarization,} \quad (11)$$

permits us to state easily the boundary conditions from the elementary laws of electromagnetism: ψ must be continuous on each interface $u = u_j$ $(j = 0, Q)$.

The first problem stated in Section 2 reduces in the new coordinate system to the solution of Eqs. (9) and (10) with continuity conditions for ψ. The OWC can be derived from Eqs. (6) and (8): when $y \to \infty$, the field $F(x, u)$ must be the sum of the two right-hand members of these equations.

D. Solution of the Mathematical Problem

The problem stated in the previous section will be solved by using Eqs. (9) and (10), successively, then continuity conditions, then OWC's.

Using Maxwell's Equations

It is important to notice in Eqs. (9) and (10) that the function $a(x)$ appears only through the two periodic functions

$$\mathcal{C}(x) = \frac{1}{1+a'^2}, \qquad \mathcal{D}(x) = \frac{a'}{1+a'^2},$$

which can be expanded in Fourier series:

$$\mathcal{C}(x) = \sum_p \mathcal{C}_p \exp(ipKx), \quad (12)$$

$$\mathcal{D}(x) = \sum_p \mathcal{D}_p \exp(ipKx). \quad (13)$$

We are then led by the Floquet–Bloch theorem to look for solutions of Eqs. (9) and (10) having the following form:

$$F = \sum_m F_m(u)\exp(i\alpha_m x), \quad (14)$$

$$G = \sum_m G_m(u)\exp(i\alpha_m x),$$

$$\psi = \sum_m \psi_m(u)\exp(i\alpha_m x), \quad (15)$$

Introducing the right-hand sides of Eqs. (12)–(15) in Eqs. (9) and (10) permits us to obtain an infinite system of linear differential equations of the first order with constant coefficients in each medium j:

$$-i\frac{\partial F_m}{\partial u} = \sum_p (\alpha_p\mathcal{D}_{m-pFp} + \mathcal{C}_{m-pGp}), \quad (16)$$

$$-i\frac{\partial G_m}{\partial u} = \sum_p [(-\alpha_m\alpha_p\mathcal{C}_{m-p} + k^2\nu_j^2\delta_{mp})F_p + \alpha_m\mathcal{D}_{m-pGp}], \quad (17)$$

where δ_{mp} denotes the Kronecker symbol.

For the sake of simplicity, it is useful to introduce a generalized vector $\xi(u)$ having a double infinity of components, which is the limit when $N \to \infty$ of the vector $\gamma_N(u)$:

$$\gamma_N = (F_{-N}, F_{-N+1}, \ldots F_N, G_{-N}, G_{-N+1}, \ldots, G_N) \quad \text{for TE polarization,} \quad (18)$$

$$\gamma_N = [F_{-N}, \ldots, F_N, G_{-N}/\nu^2(u), \ldots, G_N/\nu^2(u)] \quad \text{for TM polarization,} \quad (19)$$

where the function $\nu(u)$ is a piecewise constant function, equal to the index ν_j for the ordinate u. With these new notations, Eqs. (16) and (17) yield, in each medium j,

$$-i\frac{d\xi}{du} = \{[R(u)]^{-1}T(u)R(u)\}\xi, \quad (20)$$

where $T(u)$ is a generalized matrix defined, like vector ξ, by the limit when $N \to \infty$ of a matrix

$$\begin{pmatrix} A & B \\ C & D \end{pmatrix},$$

[A–D being four matrices of size $2N + 1$ given for m and $n \in (-N, +N)$] by

$$A_{m,n} = \alpha_n\mathcal{D}_{m-n},$$
$$B_{m,n} = \mathcal{C}_{m-n},$$
$$C_{m,n} = -\alpha_m\alpha_n\mathcal{C}_{m-n} + k^2\nu_j^2(u)\delta_{mn},$$
$$D_{m,n} = \alpha_m\mathcal{D}_{m-n}.$$

R is a generalized diagonal matrix

$$\begin{pmatrix} R_1 & 0 \\ 0 & R_2 \end{pmatrix},$$

the limit for $N \to \infty$ of a matrix obtained by juxtaposition of four matrices of size $2N + 1$: the 0 matrix, the R_1 matrix [of component δ_{mn} for the TE case or $\delta_{mn}/\nu(u)$ for the TM case] and the R_2 matrix [of component δ_{mn} for the TE case or $\delta_{mn}\nu(u)$ for the TM case]. $(R)^{-1}$ is obtained simply by interchanging R_2 and R_1 in R.

Bearing in mind the conditions of continuity of ψ, it is interesting to notice that Eq. (20) is valid in the sense of distri-

butions since ξ is continuous on each interface. Also, this equation remains valid in the more complicated case in which $\nu(u)$ is not piecewise constant but is an arbitrary function of u.

Now since $R^{-1}TR$ contained in the right-hand member of Eq. (20) is constant in each medium j, we can expand $\xi(u)$ as a sum of exponentials in medium j,

$$\xi(u) = \sum_{q=1}^{\infty} \xi_q{}^j \exp(ir_q{}^j u), \tag{21}$$

where $r_q{}^j$ are the eigenvalues of matrix $R^{-1}TR$ (the same as those of T) and where $\xi_q{}^j$ are proportional to the eigenvectors $R^{-1}V_q{}^j$ of matrix $R^{-1}TR$, $V_q{}^j$ being the corresponding eigenvectors of T,

$$\xi_q{}^j = b_q{}^j(R^{-1}\mathbf{V}_q{}^j). \tag{22}$$

Finally, from Eqs. (21) and (22) we derive the form of $\xi(u)$ in each medium j,

$$\xi = M^j\phi^j(u)\mathbf{b}^j, \tag{23}$$

where $\mathbf{b}^j$ is a vector of components $b_q{}^j$ from $q = 1$ to $q = \infty$, $\phi^j(u)$ is the diagonal matrix of components $\phi_{qp}{}^j = \exp(ir_q{}^j u)\delta_{qp}$, and M is a matrix whose columns are the vectors $(R^{-1}\mathbf{V}_q{}^j)$ from $q = 1$ to $q = \infty$. From ξ, we can deduce the fields. The problem reduces now to the search for vectors $\mathbf{b}^j$ in each medium.

Using Boundary Conditions

From the continuity of $\xi(u)$ at each interface u_j, we derive $V_j \in (0, Q)$:

$$M^j\phi^j(u_j)\mathbf{b}^j = M^{j+1}\phi^{j+1}(u_j)\mathbf{b}^{j+1}. \tag{24}$$

From these relations, and noting that

$$\phi^j(u_j)[\phi^j(u_{j-1})]^{-1} = \phi^j(u_j - u_{j-1}) = \phi^j(e_j),$$
$$\phi^{Q+1}(u_Q) = \phi^{Q+1}(0) = 1,$$

where 1 is the unit diagonal matrix, we finally deduce a relation between $\mathbf{b}^0$ and $\mathbf{b}^{Q+1}$:

$$M^{Q+1}\mathbf{b}^{Q+1} = [M^Q\phi^Q(e_Q)(M^Q)^{-1}]\ldots[M^j\phi^j(e_j)(M^j)^{-1}]$$
$$\ldots[M^1\phi^1(e_1)(M^1)^{-1}]\,M^0\phi^0(-e)\mathbf{b}^0. \tag{25}$$

For a noncoated grating (Q = 0), Eq. (25) becomes

$$M^0\mathbf{b}^0 = M^1\mathbf{b}^1.$$

On the other hand, for a multicoated grating, it is worth noting that in Eq. (25) each medium j is represented by the matrix $H^j = M^j\phi^j(e_j)(M^j)^{-1}$; hence Eq. (25) can be written in the form

$$H\mathbf{b}^0 = M^{Q+1}\mathbf{b}^{Q+1}, \tag{26}$$

with

$$H = H^QH^{Q-1}\ldots H^1M^0\phi^0(-e).$$

The user is generally interested in the field above the grating, represented by the vector $\mathbf{b}^{Q+1}$. Equation (26) gives a relation between $\mathbf{b}^{Q+1}$ and $\mathbf{b}^0$, $\mathbf{b}^0$ representing the field in the substrate. Now, to determine $\mathbf{b}^{Q+1}$, we shall use the outgoing-wave condition.

Outgoing-Wave Condition

We have to introduce new conditions on vectors $\mathbf{b}^0$ and $\mathbf{b}^{Q+1}$ of Eq. (26). Indeed, in the substrate, the field must satisfy the outgoing-wave condition. This means that we must keep in $\mathbf{b}^0$ only the components $b_q{}^0$ for which $r_q{}^0$ corresponds to a wave whose amplitude decreases for $y \to -\infty$ or is propagating downward. Since the u dependence of this wave is in $\exp(ir_q{}^0u)$, we obviously must keep only $r_q{}^0$ such that

$$\mathrm{Im}(r_q{}^0) < 0, \quad \text{or} \quad \mathrm{Im}(r_q{}^0) = 0 \quad \text{and} \quad \mathrm{Re}(r_q{}^0) < 0. \tag{27}$$

The outgoing-wave condition in vacuum could be expressed in a similar manner. In fact, for numerical reasons, we have been led to separate the incident and asymptotic diffracted fields from the evanescent diffracted field, the former being given by Eqs. (6) and (8) and the latter being the only one to be expressed as a sum of exponentials as in Eq. (21).

Therefore Eq. (23) must be replaced for $j = Q + 1$ by

$$\xi = M^{Q+1}\phi^{Q+1}(u)\mathbf{b}^{Q+1} + \exp(-i\beta_0 u)\mathbf{l} + M'\phi'(u)\mathbf{B},$$

where $\mathbf{l}$ is a generalized vector having a double infinity of components, the limit when $N \to \infty$ of the vector

$$\begin{pmatrix} \mathbf{l}' \\ \mathbf{l}'' \end{pmatrix}$$

given for $m \in (-N, +N)$ by[6]

$$\mathbf{l}'_m = L_m(\beta_0),$$
$$\mathbf{l}''_m = -\left(\beta_0 - mK\frac{\alpha_0}{\beta_0}\right)L_m(\beta_0),$$

$\mathbf{B}$ a vector of components B_n ($n \in U$) and of size P, $\phi'(u)$ a diagonal matrix of size P and components $\exp(i\beta_n u)\delta_{nm}$, and M' a generalized matrix, the limit when $N \to \infty$ of a rectangular matrix

$$\begin{pmatrix} M'' \\ M''' \end{pmatrix},$$

M'' and M''' being rectangular matrices of size $(4N + 2) \times P$ given for $m \in (-N, +N)$ and $n \in U$ by

$$M''_{mn} = L_{m-n}(-\beta_n),$$
$$M'''_{mn} = [\beta_n - (m - n)K\alpha_n/\beta_n]L_{m-n}(-\beta_n).$$

As a consequence, Eq. (26) now becomes

$$H\mathbf{b}^0 = M^{Q+1}\mathbf{b}^{Q+1} + \mathbf{l} + M'\mathbf{B}. \tag{28}$$

Since the term $M^{Q+1}\mathbf{b}^{Q+1}$ represents only the evanescent diffracted field, the outgoing-wave condition in vacuum can be easily expressed: We must keep only the components of $\mathbf{b}^{Q+1}$ corresponding to $r_q{}^{Q+1}$ such that

$$\mathrm{Im}(r_q{}^{Q+1}) > 0. \tag{29}$$

We prove in Section 4 that Eq. (28) enables us to calculate the unknown vectors $\mathbf{b}$, $\mathbf{b}^{Q+1}$, and $\mathbf{B}$.

4. NUMERICAL APPLICATION

A. Truncation

The numerical application requires the truncation of all the matrices and vectors contained in Eq. (28). So we replace the

infinite vector ξ of Eq. (20) by the finite vector γ_n given by Eqs. (18) and (19), of size $2(2N+1)$. Under these conditions, the matrix T of Eq. (20) has a size $4N+2$, and we compute in each medium its $4N+2$ eigenvectors $V_q{}^j$ of size $4N+2$. From the form of the T matrix, it can be shown[6] that the number of values of $r_q{}^0$ satisfying Eq. (27) is equal to $2N+1$. Thus the number of components of $\mathbf{b}_0$ will be exactly equal to $2N+1$. In the same way, the number of $r_j{}^{Q+1}$ satisfying $\mathrm{Im}(r_j{}^{Q+1}) > 0$, or $\mathrm{Im}(r_j{}^{Q+1}) = 0$ and $\mathrm{Re}(r_j{}^{Q+1}) > 0$, is equal to $2N+1$. Furthermore, as we will see in Section 5, the number of $r_j{}^{Q+1}$ such that $\mathrm{Im}(r_j{}^{Q+1}) > 0$ is equal to $2N+1-P$. So the number of components of $\mathbf{b}^{Q+1}$ is equal to $2N+1-P$. Thus, since $\mathbf{B}$ has P components, Eq. (28) is nothing but a linear system of $4N+2$ equations with $4N+2$ unknowns, which can be solved with a classical numerical method. This permits us to know $\mathbf{b}^0$, $\mathbf{b}^{Q+1}$, and $\mathbf{B}$. The values of $\mathbf{b}^j$ in each medium can be deduced from Eq. (24).

The computer code that we have constructed permits us to obtain short computation times of the order of some seconds on a CDC 7600 computer. It must be noticed that this rough estimate must be increased for gratings having a large number of coatings and that it corresponds to a number N close to 10 that has been generally adopted for the results described in Section 5.

B. Remarks

By identification of the u dependence in Eqs. (8) and (21) it turns out that, when $N \to \infty$, P values $r_q{}^{Q+1}$ must tend toward the P values of β_n corresponding to $n \in U$. More generally, it is easy to see that, when $N \to \infty$, a finite number $4N'+2$ values of $r_q{}^{Q+1}$ ($P < N' < N$) tend toward the β_n and β_{-n} ($-N' < n < +N'$). So it could seem advantageous to use the analytic solution for $N = \infty$ of the problem of the eigenvalues and eigenvectors of T. Surprisingly, if we operate in such a way, we can show that this method is equivalent to the well-known Rayleigh expansion method,[1] which generally leads to a numerical failure. To explain this paradoxical result, we have to point out that, after truncation, the $r_q{}^{Q+1}$ will be different from the β_n and $-\beta_n$, contrary to what happens in the numerical application of the Rayleigh method. So the two theories, which appear to be close to each other before truncation, are quite different in the numerical application. The reader will find in Table 1 the values of β_n and $r_q{}^{Q+1}$ obtained in the case of a sinusoidal grating. However, it is possible to carry out the calculation without separation between the two kinds of fields. In this case, the efficiencies are computed like the probabilities of states in quantum mechanics.[2,6]

Table 1. Comparison of the Values of β_n (for $n \geq 0$) and $r_q{}^{Q+1}$ Obtained for a Sinusoidal Grating of Groove Depth $h = 4$ μm and Groove Spacing $d = 18$ μm Illuminated under Normal Incidence with the Wavelength $\lambda = 10$ μm, the Truncation Being Made with $N = 10$

n	$\mathrm{Re}(\beta_n)/k$	$\mathrm{Im}(\beta_n)/k$	$\mathrm{Re}(r_q{}^{Q+1})/k$	$\mathrm{Im}(r_q{}^{Q+1})/k$
0	1.0000000	0	1.0000000	0
1	0.83147942	0	0.83147942	0
2	0	0.48432210	0	0.48432210
3	0	1.3333333	0	1.3333333
4	0	1.9845079	0	1.9844902
5	0	2.5915342	0	2.6080262
6	0	3.1797973	0	2.8792848
7	0	3.7581188	3.1513533	0.6576725
8	0	4.3304834	−3.1513533	0.6576725
9	0	4.8989795	3.5123515	1.5417451
10	0	5.4648145	−3.5123515	1.5417451

It is worth noting that the separation between evanescent and asymptotic diffracted fields could be made in the substrate, too, when this substrate is dielectric. This would permit us to compute the efficiencies in the transmitted orders of a dielectric grating.

5. APPLICATIONS

In this section, we intend to show that our computer code actually extends the possibilities of theoretical predictions in the field of diffraction gratings. To this end, we give two examples concerning recent applications of the properties of diffraction gratings.

A. Using Dielectric Coatings to Minimize the Absorption of Light by Diffraction Gratings

Highly reflecting metals, such as aluminum, silver, and gold, are traditionaly used in the construction of diffraction gratings. As a consequence, the energy absorbed by these gratings reaches 10% in the visible region and decreases in the infrared region (about 1% at 10 μm). However, this absorption is considerably enhanced if some Wood anomaly occurs.[4]

For some recent applications of gratings, this absorption must be strongly reduced. For instance, it is the case for gratings used as beam-sampling mirrors for high-power lasers.[4] These gratings generally operate at 10.6 μm and must absorb less than about 0.1% of the energy contained in the laser beam in order to avoid destruction. We know that this goal may be reached by using adequate λ/4 dielectric coatings deposited on the metallic substrate. This property is well known for metallic mirrors but unfortunately does not always hold for gratings. Indeed, the dielectric coatings multiply the number of Wood anomalies, and therefore it is impossible to have *a priori* an idea whether the multicoated grating is highly reflecting or whether it is strongly absorbing. The problem is identical for gratings used at the end of the cavity of tunable lasers in the visible region,[4,5] where a reduction of absorption can strongly enhance the performance of the laser.

At this time, the only tools that we have at hand to predict the behavior of multicoated gratings are the rigorous computer codes obtained from electromagnetic theories. To our knowledge, these computer codes are few in number, and it seems that the most powerful in the visible and infrared regions has been constructed by one of the authors, at least in the case in which all the interfaces are modulated.[8] This code has been used to perform a numerical optimization of holographic and ruled gratings coated with dielectric layers, in collaboration with an experimental study by Jobin-Yvon.[4] In practice, numerical reasons prevented the authors from achieving accurate computations as soon as the number of dielectric coatings exceeded three. Nevertheless, it appeared that a significant decrease of absorption was possible, for instance by a ratio of 2 for a 3000-groove/mm holographic grating with a sinusoidal profile, a fact qualitatively confirmed by experiments made by Jobin-Yvon.

First, we have thoroughly compared the results from the two computer codes when the number of dielectric coatings is fewer than three: the relative discrepancy does not exceed

10^{-2} and generally is of the order of 10^{-3}. Similar computations made in the infrared with gratings having a groove spacing of 18 μm illuminated with $\lambda = 10$ μm have led to similar conclusions. So, since the results obtained from the computer code by using the integral formalism can be considered as exact[8] to within 10^{-2}, we can deduce that our new computer code enables us to obtain accurate results in any region of wavelength. Classical numerical tests, such as the energy-balance criterion and the reciprocity theorem,[1] have confirmed this conclusion. This is even more remarkable since the previous differential formalism was unable to achieve accurate computations for metallic gratings above 0.6 μm because of numerical instabilities.[9] Now it is tempting to carry on the numerical study recently developed on gratings for tunable lasers[4] in order to investigate the performances of gratings coated with more than three dielectric layers. We have chosen to perform our calculations in case C of Table 1 of a previous study.[4]

The first grating, G_0, is an uncoated aluminum grating having 3000 grooves/mm with a sinusoidal profile of groove depth $h = 0.12$ μm. The second one, G_1, was obtained by coating G_0 with a stack of two dielectrics: a first layer of MgF_2 on the metallic substrate, with thickness 0.106 μm, and a second layer of TiO_2, with thickness 0.0602 μm. Taking into account the indices of MgF_2 (1.39) and TiO_2 (2.45), it is worth noting that the optical thicknesses of these two dielectric coatings represent $\lambda/4$ for $\lambda = 0.59$ μm. Finally G_2, G_3, and G_4 are obtained by depositing on G_0 two, three, and four identical stacks of two dielectric coatings.

Figure 2 shows the efficiency curves of these gratings in a Littrow mount for TM polarization. The most important conclusion is that the maximum efficiency strongly increases with the number of dielectric stacks. This is a consequence

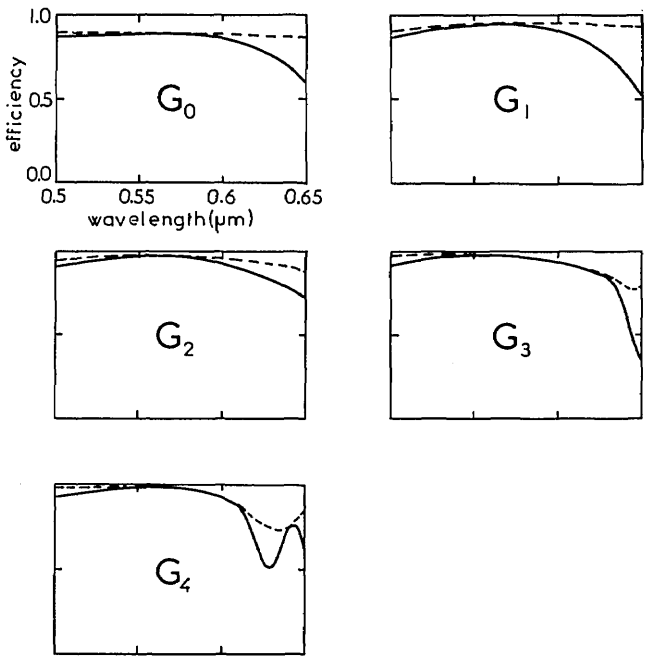

Fig. 2. Efficiency curves in a Littrow mount of a sinusoidal aluminum grating covered by 0 (for G_0), two (G_1), four (G_2), six (G_3), or eight (G_4) stacks of $\lambda/4$ dielectric layers. The dashed line corresponds to the total efficiency (0 order and -1 order) and the solid line to the efficiency in the -1 order.

of the decrease of the energy absorbed by the grating, which is equal to 12, 6, 3, 1.3, and 0.7% for G_0, G_1, G_2, G_3, and G_4, respectively. Of course, the relative precision of the values obtained for G_3 and G_4 is poor since the absorption has the same order of magnitude as the precision of the computation. Nevertheless, it is possible to state an empirical rule: Depositing a new stack of $\lambda/4$ dielectric coatings results in the decrease of absorption by a factor of 2. It is curious to notice that the blaze effect, i.e., the concentration of the incident energy in the Littrow order, which practically always coincides with the minimum of absorption, occurs for a wavelength close to 0.56 μm. Indeed, the thicknesses of dielectric have been chosen to produce a minimum absorption at 0.59 μm, at least for a mirror. It seems that this shift of the blaze wavelength is due to the absorption peak on the right of the figure, essentially for G_3 and G_4, where the absorption reaches 22 and 50% for $\lambda = 0.64$ μm and $\lambda = 0.63$ μm, respectively.

This phenomenon clearly shows that, because of the Wood anomalies, the behavior of multicoated gratings cannot be deduced from simple rules and that it is necessary to have at hand rigorous computer codes to investigate their properties.

B. Absorption of Light by Highly Modulated Gratings

Various recent applications have brought a new interest in the study of highly modulated gratings. One of these applications is the use of crossed gratings as solar-selective absorbers. In this paper, it is not our purpose to describe the characteristics and the properties of these crossed gratings. The interested reader can consult recent papers[10,11] for a review of the subject. Roughly, a crossed grating differs from the classical one by the fact that it presents a periodic modulation not only on the $0x$ axis but also on the $0z$ axis, in such a way that its profile can be described by the function $y = a(x, z)$, where $a(x, z)$ is periodic in x and z. Experimental studies[12] have shown that this kind of structure can be used as a solar-selective absorber, provided that the modulation depth is very large. A rigorous theoretical study of these structures was recently made.[10] Unfortunately, the complicated computer code that has been achieved is unable, for numerical reasons, to perform computations when the modulation depth becomes large. However, it has been possible, from this computer code, to state an empirical equivalence formula[10,11] able to deduce the properties of a class of crossed gratings such that $a(x, z) = a_1(x) + a_2(z)$, from the properties of the two classical gratings $y = a_1(x)$ and $y = a_2(z)$.

A second example of the recent applications of highly modulated gratings can be found in the use of dielectric transmission gratings in the zero-order diffraction system for recording color images as embossable surface-relief structures in transparent plastic media, as proposed by Knop. (See, for instance, a review on the subject and some theoretical calculations in Ref. 5.)

It is now important to investigate the properties of highly modulated classical gratings. For numerical reasons, the existing rigorous computer codes are practically unable to achieve accurate computations as soon as the groove depth exceeds one or two times the groove spacing. We will show that our new computer code is suitable for higher gratings.

Figures 3 and 4 show the efficiency curves of a sinusoidal aluminum grating having a groove spacing equal to 0.737 μm and illuminated with a monochromatic light $\lambda = 0.59$ μm with

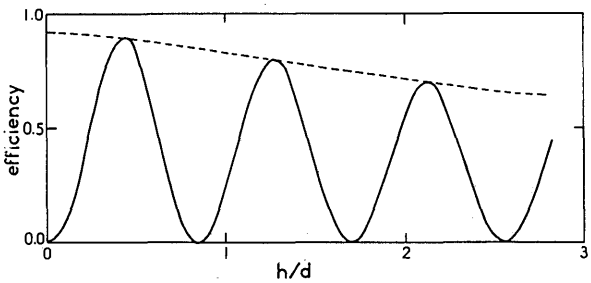

Fig. 3. Efficiency in Littrow configuration and for TE polarization of an aluminum sinusoidal grating versus the groove-depth to groove-spacing ratio h/d. The dashed line represents the total efficiency and the solid line the -1-order efficiency.

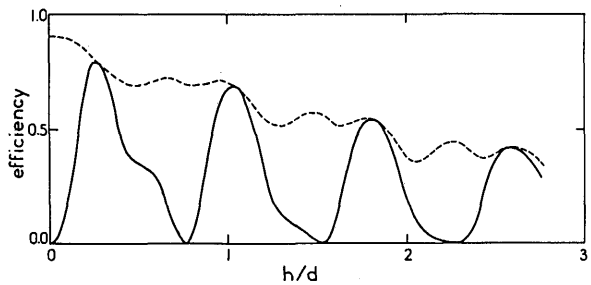

Fig. 4. The same as Fig. 3 but for TM polarization.

angle of incidence $\theta = 23.6°$. It is worth noting that only two orders (0 and -1) are diffracted and that, with the above parameters, we are in a Littrow mounting, where the -1 order has the same direction of propagation as the incident wave. The curves may be compared with those published in a recent paper,[13] corresponding to the case of a perfectly conducting grating. We can see that our computer code makes it possible to investigate the properties of gratings whose groove-depth to groove-spacing ratio is about 3. For perfectly conducting gratings, the efficiency $\mathcal{E}_{-1}$ in the -1 order was given with good accuracy by a simple formula, issued from a phenomenological theory[13]:

$$\mathcal{E}_{-1} = \sin^2 [\rho(h)],$$

where $\rho(h)$ was practically a linear function of h, depending on the polarization. This time we do not have a phenomenological theory at our disposal, since the grating is not perfectly conducting. Nevertheless, from Figs. 3 and 4, it seems that the shape of the efficiency curves strongly depends on the polarization. For TE polarization, the total efficiency $\Sigma\mathcal{E}$ can be represented practically by a straight line, and the efficiency in the -1 order is practically a sinusoid with a decreasing amplitude:

$$\mathcal{E}_{-1} = \Sigma\mathcal{E} \sin^2 [\rho(h)],$$

$\rho(h)$ being nearly the same as for the perfectly conducting grating. This conclusion no longer holds for TM polarization. In this case, $\mathcal{E}_{-1}$ oscillates, but the curve differs considerably from a sinusoid. Furthermore, the total efficiency roughly decreases with h but with oscillations having a frequency different from that of $\mathcal{E}_{-1}$. Another big difference between the two polarizations lies in the importance of the absorption, which reaches 0.65 for TM polarization and only 0.35 for TE polarization, when the groove-depth to groove-spacing ratio is close to 3. For both polarizations, we can notice that the efficiency $\mathcal{E}_{-1}$ oscillates between perfect zeros and perfect blazings (where $\mathcal{E}_0$ is equal to zero).

Figures 5 and 6 show similar curves for a non-Littrow mount. The sinusoidal aluminum grating with groove spacing 0.333 μm is illuminated with wavelength 0.59 μm with an angle of incidence of 55° in such a way that only two orders are diffracted. In the right-hand side of the figure, the groove-depth to groove-spacing ratio is equal to 6. For TE polarization, the frequency of the oscillations is very low, and we cannot observe the first maximum of the curve. For TM polarization, the curve oscillates strongly, but it is worth noting that perfect zeros and perfect blazings completely disappear.

To our knowledge, this is the first time that a computer code able to deal with gratings of arbitrary profile can achieve accurate computations for such highly modulated gratings.

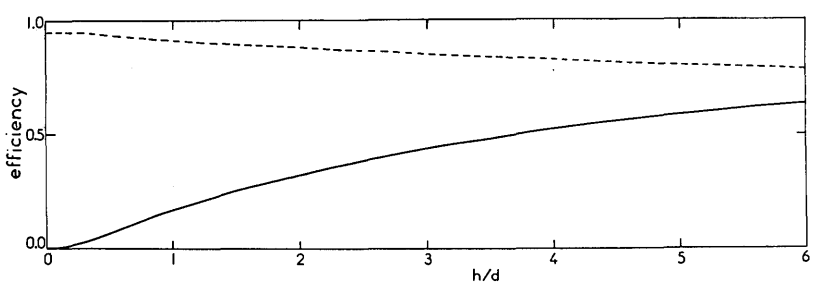

Fig. 5. Efficiency in a non-Littrow configuration and for TE polarization of an aluminum grating versus the groove-depth to groove-spacing ratio h/d. The dashed line represents the total efficiency and the solid line the -1-order efficiency.

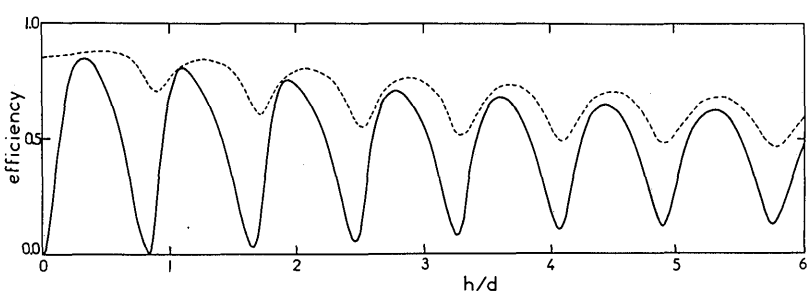

Fig. 6. The same as Fig. 5 but for TM polarization.

6. CONCLUSIONS

We have described a new differential formalism for multicoated diffraction gratings. It extends the domain of application of the differential formalism to the metallic gratings used in the visible and infrared regions, but it also permits us to investigate, for the first time, the properties of gratings covered with a great number of modulated layers or the behavior of highly modulated gratings of arbitrary shape.

By using this new computer code, we can find answers to problems concerning the traditional use of gratings in any region or wavelength. In addition, we can investigate the properties of new kinds of gratings used for recent applications.

REFERENCES

1. R. Petit, ed., *Electromagnetic Theory of Gratings* (Springer-Verlag, Berlin, 1980): R. Petit, Chap. 1, pp. 1–52; D. Maystre, Chap. 3, pp. 63–100; P. Vincent, Chap. 4, pp. 101–121.
2. J. Chandezon, D. Maystre, and G. Raoult, "A new theoretical method for diffraction gratings and its numerical application," J. Opt. (Paris) **11**, 235–241 (1980).
3. E. J. Post, *Formal structure of Electromagnetics* (North-Holland, Amsterdam, 1962), pp. 144–159.
4. D. Maystre, J. P. Laude, P. Gacoin, D. Lepère, and J. P. Priou, "Gratings for tunable lasers: using multidielectric coatings to improve their efficiency," Appl. Opt. **19**, 3099–3102 (1980).
5. D. Maystre, M. Nevière, and R. Petit, in *Electromagnetic Theory Of Gratings*, R. Petit, ed. (Springer-Verlag, Berlin, 1980), Chap. 6, pp. 159–225.
6. J. Chandezon, "Les equatians de Maxwell sous forme covariante. Application à l'étude de la propagation dans les guides periodques et à la diffraction par les reseaux," Ph.D. Thesis (Clermont-Ferrand University, Aubiere, France, 1979).
7. In this usual mounting, there is a certain value of n for which the nth-diffracted wave and the incident wave are propagating in opposite directions, so $\beta_n = \beta_0$.
8. D. Maystre, "A new general integral theory for dielectric coated gratings," J. Opt. Soc. Am. **68**, 490–495 (1978).
9. M. Nevière, P. Vincent, and R. Petit, "Theory of conducting gratings and their applications to optics," Nouv. Rev. Opt. **5**, 65–77 (1974).
10. G. H. Derrick, R. C. McPhedran, D. Maystre, and M. Nevière, "Crossed gratings: a theory and its applications," Appl. Phys. **18**, 39–51 (1979).
11. R. C. McPhedran, G. H. Derrick, and L. C. Botten, in *Electromagnetic Theory of Gratings*, R. Petit, ed. (Springer-Verlag, Berlin, 1980), Chap. 7, pp. 227–276.
12. P. B. Clapham and M. C. Hutley, "Reduction of lens reflexion by the 'moth eye' principle," Nature **244**, 281–282 (1973).
13. D. Maystre, M. Cadilhac, and J. Chandezon, "Gratings: a phenomenological approach and its applications, perfect blazing in a non-zero deviation mounting," Opt. Acta **28**, 457–470 (1981).